Photocurrent Generation under a Large Dipole Moment Formed by Self-Assembled Monolayers of Helical Peptides Having an *N*-Ethylcarbazolyl Group

Tomoyuki Morita, Shunsaku Kimura,* and Shiro Kobayashi

Contribution from the Department of Material Chemistry, Graduate School of Engineering, Kyoto University, Yoshida Honmachi, Sakyo-ku, Kyoto 606-8501, Japan

Yukio Imanishi

Graduate School of Materials Science, Nara Institute of Science and Technology, 8916-5 Takayama-cho, Ikoma, Nara 630-0101, Japan

Received August 3, 1999

Abstract: Self-assembled monolayers (SAMs) of α-helical peptides carrying an *N*-ethylcarbazolyl (ECz) group were prepared. The helical peptide SAMs on a gold surface were characterized by quartz crystal microbalance measurements, cyclic voltammetry, and impedance spectroscopy, showing that a tridecapeptide SAM with the N-terminal binding to gold was packed more densely than that with the C-terminal binding. The helix tilt angles from the surface normal in these peptide SAMs were found to be about 40° on the basis of Fourier transform infrared reflection−absorption spectroscopy. Photocurrent generation of these peptide SAMs in an aqueous solution was investigated by photoexcitation of ECz groups either in the presence of an electron donor or acceptor. In the presence of methyl viologen (electron acceptor), electron donation from a gold surface to an ECz group was observed upon photoexcitation. On the other hand, in the presence of triethanolamine or ethylenediaminetetraacetic acid (electron donor), the direction of photocurrent was reversed. In the case of the anodic photocurrent generation using triethanoamine, the electron donation from an ECz group to a gold surface was accelerated by the helix dipole moment directing toward a gold surface. Furthermore, the electronic coupling between an ECz group and a gold surface through the peptide molecule was found to occur more strongly than that through a saturated hydrocarbon. The helical peptides were therefore shown to be an excellent medium for electron transfer.

Introduction

In the natural photosynthesis, long-range electron transfer between a donor and an acceptor chromophore in protein assemblies occurs efficiently.[1−3] It has been shown that the electrostatic field generated by the dipole moment of α-helical segments of proteins accelerates electron transfer effectively.[4,5] A peptide backbone, which is composed of π and n (nonbonding) orbitals, is also suggested to construct electron-transfer pathways,[6−8] and a donor chromophore might be electronically coupled with an acceptor chromophore through hydrogen bonds involved in an α-helix structure.[9] Therefore, α-helical peptide is expected to be an excellent medium for electron transfer. In the present study, self-assembled monolayers (SAMs) composed of α-helical peptides on a gold substrate were prepared and photocurrent generation therein was investigated.

It is well established that thiol and disulfide compounds are covalently connected to a gold surface via an S−Au linkage, forming highly ordered SAMs.[10] Taking advantage of this structural regularity, photocurrent generation using SAMs has been studied extensively.[11−16] However, photocurrent generation by peptide SAMs has not been reported so far. In the present investigation, we synthesized four novel kinds of disulfide compounds including helical peptides as shown in Figure 1 together with their abbreviations. An alternating sequence of L-alanine (Ala) and α-aminoisobutyric acid (Aib) was chosen for the peptide backbone because of its high preference for adopting a helical structure.[17−19] ECz-A12-SS is a tridecapeptide carrying an *N*-ethylcarbazolyl (ECz) group at the N-terminal

(1) Beratan, D. N.; Onuchic, J. N.; Hopfield, J. J. *J. Phys. Chem.* **1987**, *86*, 4488.
(2) Closs, G. L.; Miller, J. R. *Science* **1988**, *240*, 440.
(3) McDermott, G.; Prince, S. M.; Freer, A. A.; HawthornthwaiteLawless, A. M.; Papiz, M. Z.; Cogdell, R. J.; Isaacs, N. W. *Nature* **1995**, *374*, 517.
(4) Hol, W. G. *J. Prog. Biophys. Mol. Biol.* **1985**, *45*, 149.
(5) Galoppini, E.; Fox, M. A. *J. Am. Chem. Soc.* **1996**, *118*, 2299.
(6) Evans, M. G.; Gergeley, J. *Biochim. Biophys. Acta* **1949**, *3*, 188.
(7) Halpern, J.; Orgel, L. E. *Discuss. Faraday Soc.* **1960**, *29*, 32.
(8) Isied, S. S.; Ogawa, M. Y.; Wishart, J. F. *Chem. Rev.* **1992**, *92*, 381.
(9) Gray, H. B.; Winkler, J. R. *J. Electroanal. Chem.* **1997**, *438*, 43.
(10) Ulman, A. *An Introduction to Ultrathin Organic Films*; Academic Press: San Diego, CA, 1991.
(11) Yamada, S.; Kohrogi, H.; Matsuo, T. *Chem. Lett.* **1995**, 639.
(12) Akiyama, T.; Imahori, H.; Ajawakom, A.; Sakata, Y. *Chem. Lett.* **1996**, 907.
(13) Byrd, H.; Suponeva, E. P.; Bocarsly, A. B.; Thompson, M. E. *Nature* **1996**, *380*, 610.
(14) Yamada, S.; Koide, Y.; Matsuo, T. *J. Electroanal. Chem.* **1997**, *426*, 23.
(15) Uosaki, K.; Kondo, T.; Zhang, X.-Q.; Yanagida, M. *J. Am. Chem. Soc.* **1997**, *119*, 8367.
(16) Imahori, H.; Norieda, H.; Ozawa, S.; Ushida, K.; Yamada, H.; Azuma, T.; Tamaki, K.; Sakata, Y. *Langmuir* **1998**, *14*, 5335.
(17) Otoda, K.; Kitagawa, Y.; Kimura, S.; Imanishi, Y. *Biopolymers* **1993**, *33*, 1337.
(18) Fujita, K.; Kimura, S.; Imanishi, Y.; Rump, E.; Ringsdorf, H. *Langmuir* **1994**, *10*, 2731.
(19) Miura, Y.; Kimura, S.; Imanishi, Y.; Umemura, J. *Langmuir* **1998**, *14*, 6935.

10.1021/ja992769l CCC: $19.00
Published on Web 03/11/2000

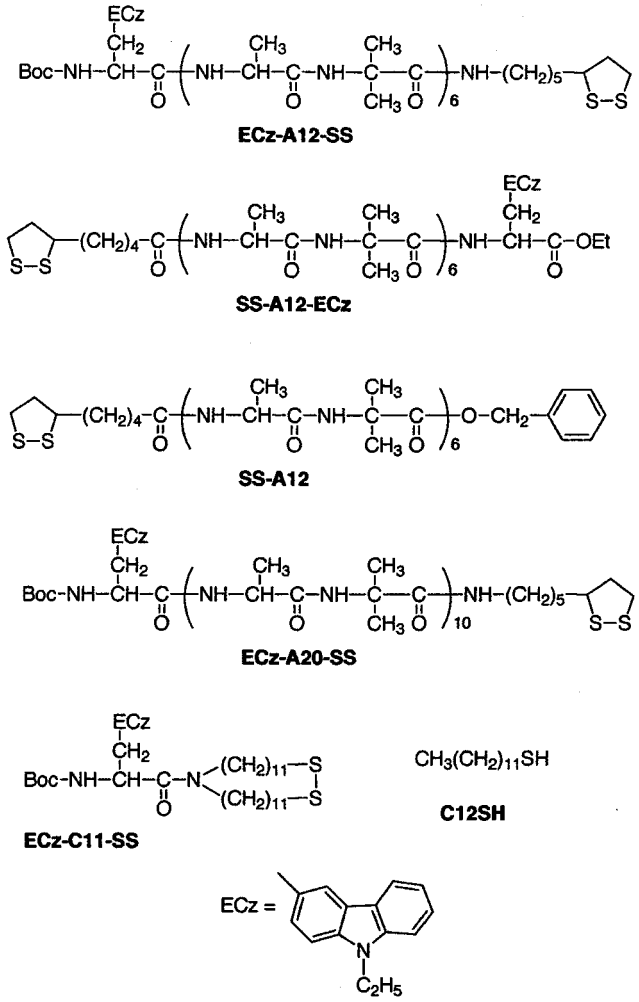

Figure 1. Molecular structures of newly synthesized disulfide compounds (ECz-A12-SS, SS-A12-ECz, ECz-A20-SS, and ECz-C11-SS) and reference compounds (SS-A12 and C12SH).

and a disulfide group at the C-terminal. The ECz group acts as a photosensitizer in this system and is useful to avoid excimer formation even in a condensed phase. The excimer formation significantly decreases the redox capability of the excited ECz group.[20−22] SS-A12-ECz is also a tridecapeptide but carries the two functional groups at the terminals in the opposite way to the case of ECz-A12-SS. ECz-A20-SS is a heneicosapeptide analogous to ECz-A12-SS in terms of the positions of the functional groups. ECz-C11-SS is a disulfide compound carrying a dialkyl chain instead of a peptide chain. SS-A12 and 1-dodecanethiol (C12SH), which do not carry ECz group, were used as control compounds.

The surface coverage of the SAMs was investigated by quartz crystal microbalance measurements, cyclic voltammetry, and impedance spectroscopy, and the molecular orientation of the peptide monolayer was determined by Fourier transform infrared reflection−absorption spectroscopy. The photocurrent generation by the SAMs was investigated, and the influence of the dipole moment, length, and structure of the linker between a gold surface and an ECz group on the rate of electron transfer was discussed.

Experimental Section

Materials. Methyl viologen trihydrate (MV^{2+}), triethanolamine (TEOA), and ethylenediaminetetraacetic acid tetrasodium salt (EDTA) were purchased from Nacalai Tesque Co., Ltd. (Japan) and used without further purification. 1-Dodecanethiol was purchased from Tokyo Kasei Co., Ltd. (Japan). Novel disulfide compounds were synthesized according to Scheme 1. All peptides were synthesized by the conventional liquid-phase method. L-3-(3-*N*-ethylcarbazolyl)alanine (ECzAla),[21] Boc-(Ala-Aib)$_2$-OH (BA4OH), Boc-(Ala-Aib)$_4$-OH (BA8OH)[23] and SS-A12[19] were synthesized as previously reported. All intermediates and final products were identified by ^{1}H NMR (270 MHz), and their purity was checked by thin-layer chromatography (TLC). The final products were confirmed by mass spectroscopy. Solvent systems for TLC were (A) chloroform/methanol/acetic acid (90/10/3 v/v/v), (B) chloroform/methanol/acetic acid (95/5/3 v/v/v), (C) chloroform/methanol/ammonia water (13/5/1 v/v/v), (D) chloroform/methanol (9/2 v/v).

***N*$^{\alpha}$-(*tert*-Butyloxycarbonyl)-L-3-(3-*N*-ethylcarbazolyl)alanine [Boc-ECzAla].** ECzAla (173 mg) was reacted with di-*tert*-butyl carbonate (240 mg) with $NaHCO_3$ (100 mg) in water (10 mL)/dioxane (20 mL) at 0 °C for 2 h and thereafter at 25 °C for 4 h. The solvent was evaporated, and *n*-hexane was added to precipitate the reaction product (110 mg, 46.9% yield). TLC: R_f(A) = 0.65, R_f(C) = 0.57. ^{1}H NMR (270 MHz, $CDCl_3$): δ (ppm) 1.37 (9H, s, $(CH_3)_3C$), 1.46 (3H, t, NCH_2CH_3), 3.26 (2H, d, $NHCHCH_2$), 4.27 (2H, q, NCH_2CH_3), 4.94 (1H, q, $NHCHCH_2$), 7.20−8.14 (7H, carbazolyl-*H*).

L-3-(3-*N*-Ethylcarbazolyl)alanine Ethyl Ester [ECzAla-OEt]. ECzAla (90 mg) was dissolved in ethanol (100 mL), and the solution was stirred at 0 °C for 2 h in the presence of hydrogen chloride. The reaction product was obtained by evaporation (66 mg, 67.8% yield). TLC: R_f(A) = 0.38, R_f(C) = 0.93. ^{1}H NMR (270 MHz, $CDCl_3$): δ (ppm) 1.07 (3H, t, $COOCH_2CH_3$), 1.38 (3H, t, NCH_2CH_3), 3.55 (2H, d, NH_2CHCH_2), 4.06 (2H, q, $COOCH_2CH_3$), 4.26 (2H, q, NCH_2CH_3), 4.38 (1H, q, NH_2CHCH_2), 7.20−8.14 (7H, carbazolyl-*H*).

1,2-Dithia-3-(1-amino-*n*-pentyl)cyclopentane [A]. DL-α-Lipoamide (1000 mg) was dissolved in tetrahydrofuran (100 mL). The solution was added to dispersion of $LiAlH_4$ (826 mg) in tetrahydrofuran (50 mL), and the reaction solution was refluxed at 70 °C for 12 h. Distilled water (8 mL) was added, and the solution was stirred at 0 °C for 30 min. After evaporation of solvent, methanol was added and the insoluble solid was removed. The supernatant was evaporated, and distilled water (100 mL) was added. The pH of the solution was adjusted to 6.5 with 1 N hydrochloric acid, and the solution was stirred at room temperature for 24 h. The reaction product was extracted with *n*-butanol and washed with 1 N aqueous NaOH solution and 1 N hydrochloric acid. The reaction product was obtained by solvent evaporation (396 mg, 42.5% yield). TLC: R_f(A) = 0.18, R_f(C) = 0.50. ^{1}H NMR (270 MHz, $CDCl_3$): δ (ppm) 1.48 (4H, m, $NH_3^+CH_2CH_2CH_2CH_2CH_2$), 1.64 (4H, m, $NH_3^+CH_2CH_2CH_2CH_2CH_2$), 1.89, 2.47 (2H, m, $CHCH_2CH_2SS$), 2.88 (2H, t, $NH_3^+CH_2CH_2CH_2CH_2CH_2$), 3.15 (2H, m, $CHCH_2CH_2SS$), 3.58 (1H, m, $CHCH_2CH_2SS$). MS (GC): *m*/*z* 191 (calcd for $C_8H_{17}NS_2$ [M^+] *m*/*z* 191.08).

BA4-SS. BA4OH (240 mg) was dissolved in dimethylformamide (6 mL), and was reacted with 1,2-dithia-3-(1-amino-*n*-pentyl)cyclopentane (254 mg) in the presence of *O*-(7-azabenzotriazol-1-yl)-1,1,3,3-tetramethyluronium hexafluorophosphate (HATU) (318 mg) with *N*,*N*-diisopropylethylamine (DIEA) (436 μL) at 0 °C for 10 min and thereafter at 25 °C for 24 h. The solvent was removed and the remaining solid was purified by a Sephadex LH-20 column using methanol as eluant (171 mg, 51.0% yield). TLC: R_f(A) = 0.60, R_f(C) = 0.75. ^{1}H NMR (270 MHz, $CDCl_3$): δ (ppm) 1.35−1.60 (31H, brm, $NHCH(CH_3)CONHC(CH_3)_2$, $NHCH_2CH_2CH_2CH_2CH_2$, $(CH_3)_3C$), 1.63 (4H, m, $NHCH_2CH_2CH_2CH_2CH_2$), 1.85, 2.41 (2H, m, $CHCH_2CH_2SS$), 3.13 (2H, m, $CHCH_2CH_2SS$), 3.17 (2H, brs, $NHCH_2CH_2CH_2CH_2CH_2$), 3.53 (1H, m, $CHCH_2CH_2SS$), 3.87, 4.06 (2H, m, $NHCH(CH_3)CONHC(CH_3)_2$), 5.53 (1H, s, $NHCH_2CH_2CH_2CH_2CH_2$), 6.73, 6.99, 7.51 (4H, s, $NHCH(CH_3)CONHC(CH_3)_2$). MS (FAB, matrix; nitrobezyl alcohol): *m*/*z* 604 (calcd for $C_{27}H_{50}N_5O_6S_2$ [$(M + H)^+$] *m*/*z* 604.31).

(20) Nakamura, H.; Fujii, H.; Sakaguchi, H.; Matsuo, T.; Nakashima, N.; Yoshihata, K.; Ikeda, T.; Tazuke, S. *J. Phys. Chem.* **1988**, *92*, 6151.
(21) Taku, K.; Sasaki, H.; Kimura, S.; Imanishi, Y. *Amino Acids* **1994**, *7*, 311.
(22) Morita, T.; Kimura, S.; Imanishi, Y. *J. Am. Chem. Soc.* **1999**, *121*, 581.
(23) Otoda, K.; Kimura, S.; Imanishi, Y. *Biochim. Biophys. Acta* **1993**, *1145*, 33.

Scheme 1. Synthetic Scheme of ECz-A12-SS, SS-A12-ECz, ECz-A20-SS, and ECz-C11-SS

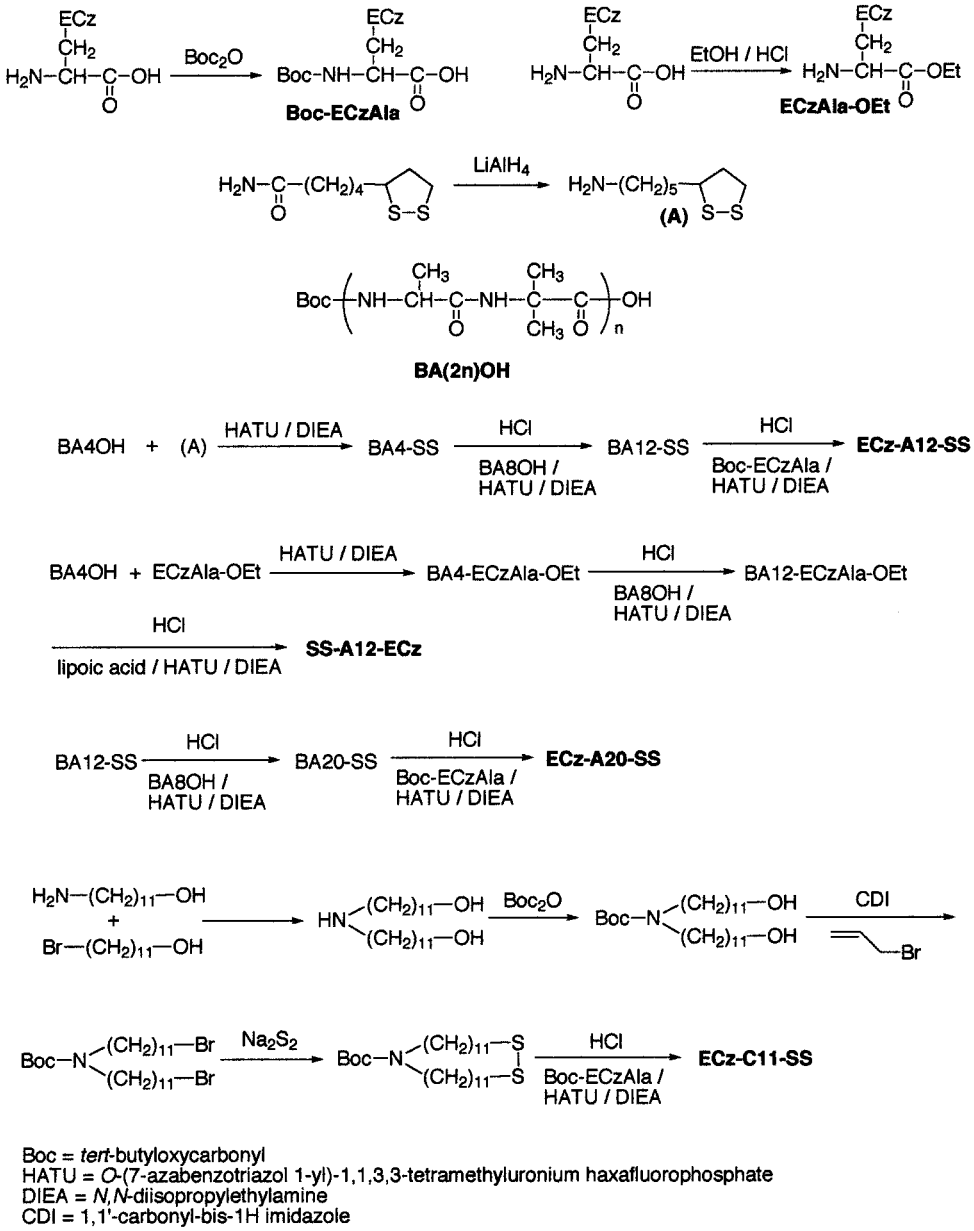

Boc = *tert*-butyloxycarbonyl
HATU = *O*-(7-azabenzotriazol 1-yl)-1,1,3,3-tetramethyluronium haxafluorophosphate
DIEA = *N,N*-diisopropylethylamine
CDI = 1,1'-carbonyl-bis-1H imidazole

BA12-SS. The Boc group of BA4-SS (42 mg) was removed by treatment with 4 N HCl in dioxane, and the product dissolved in chloroform (2 mL) was reacted with BA8OH (52 mg) in the presence of HATU (40 mg) with DIEA (27 μL) at 0 °C for 10 min and thereafter at 25 °C for 24 h. After removal of the solvent, the remaining solid was dissolved in chloroform and washed with 4 wt % $NaHCO_3$ aqueous solution and 4 wt % $NaHSO_4$ aqueous solution. The solvent was removed and the remaining solid was purified by a Sephadex LH-20 column using methanol as eluant (25 mg, 29.2% yield). TLC: R_f(A) = 0.63, R_f(C) = 0.77. ^{1}H NMR (270 MHz, $CDCl_3$): δ (ppm) 1.35−1.60 (71H, brm, NHCH(CH_3)CONHC(CH_3)$_2$, $NHCH_2CH_2CH_2CH_2CH_2$, (CH_3)$_3$C), 1.85, 2.41 (2H, m, $CHCH_2CH_2SS$), 3.13 (2H, m, $CHCH_2CH_2$-SS), 3.17 (2H, brs, $NHCH_2CH_2CH_2CH_2CH_2$), 3.53 (1H, m, $CHCH_2$-CH_2SS), 3.95, 4.24 (6H, m, NHCH(CH_3)CONHC(CH_3)$_2$), 5.68 (1H, s, N$H$$CH_2CH_2CH_2CH_2CH_2$), 7.30−7.72 (12H, s, N$H$CH($CH_3$)CON$H$C-($CH_3$)$_2$). MS (FAB, matrix; nitrobezyl alcohol): *m*/*z* 1251 (calcd for $C_{55}H_{97}N_{13}O_{14}S_2Na_1$ [(M + Na)$^+$] *m*/*z* 1250.67).

ECz-A12-SS. The Boc group of BA12-SS (25 mg) was removed by treatment with 4 N HCl in dioxane, and the product dissolved in chloroform (1 mL) was reacted with Boc-ECzAla (10 mg) in the presence of HATU (15 mg) with DIEA (10 μL) at 0 °C for 10 min and thereafter at 25 °C for 24 h. After removal of the solvent, the remaining solid was dissolved in chloroform and washed with 4 wt % $NaHCO_3$ aqueous solution and 4 wt % $NaHSO_4$ aqueous solution. The solvent was removed and the remaining solid was purified by a Sephadex LH-20 column using methanol as eluant (17 mg, 55.2% yield). TLC: R_f(A) = 0.60, R_f(C) = 0.81. ^{1}H NMR (270 MHz, $CDCl_3$): δ (ppm) 1.35−1.60 (74H, brm, NHCH(CH_3)CONHC(CH_3)$_2$, $NHCH_2CH_2CH_2CH_2CH_2$, (CH_3)$_3$C, NCH_2CH_3,), 1.85, 2.41 (2H, m, $CHCH_2CH_2SS$), 3.15−3.20 (6H, brm, $CHCH_2CH_2SS$, $NHCH_2CH_2CH_2$-CH_2CH_2, $NHCHCH_2$), 3.53 (1H, m, $CHCH_2CH_2SS$), 3.95, 4.24 (6H, m, NHCH(CH_3)CONHC(CH_3)$_2$), 4.29 (2H, q, NCH_2CH_3), 4.41 (1H, q, NHC$H$$CH_2$), 5.81 (1H, s, N$H$$CH_2CH_2CH_2CH_2CH_2$), 7.30−8.12 (20H, brm, NHCH(CH_3)CONHC(CH_3)$_2$, N$H$$CHCH_2$, carbazolyl-$H$). MS (FAB, matrix; nitrobezyl alcohol): *m*/*z* 1515 (calcd for $C_{72}H_{113}N_{15}O_{15}S_2$-$Na_1$ [(M + Na)$^+$] *m*/*z* 1514.80).

BA4-ECzAla-OEt. BA4OH (67 mg) was dissolved in dimethylformamide (2 mL) and reacted with ECzAla-OEt (54 mg) in the presence of HATU (89 mg) with DIEA (61 μL) at 0 °C for 10 min and thereafter at 25 °C for 12 h. The solvent was removed and the remaining solid was purified by a Sephadex LH-20 column using methanol as eluant (73 mg, 65.2% yield). TLC: R_f(A) = 0.65, R_f(C) = 0.78. ^{1}H NMR (270 MHz, $CDCl_3$): δ (ppm) 1.07 (3H, t, $COOCH_2CH_3$), 1.25−1.44 (21H, brm, NHCH(CH_3)CONHC(CH_3)$_2$, NCH_2CH_3), 1.49 (9H, s, (CH_3)$_3$C), 3.25 (2H, d, $NHCHCH_2$), 3.83, 4.13 (2H, m, NHCH(CH_3)CONHC(CH_3)$_2$), 4.06 (2H, q, $COOCH_2CH_3$), 4.29

(2H, q, NCH_2CH$_3$), 4.74 (1H, q, NHCHCH$_2$), 5.62 (1H, d, NHCHCH$_2$), 7.18−8.04 (11H, carbazolyl-*H*, NHCH(CH$_3$)CONHC(CH$_3$)$_2$).

BA12-ECzAla-OEt. The Boc group of BA4-ECzAla-OEt (14 mg) was removed by treatment with 4 N HCl in dioxane, and the product dissolved in chloroform (2 mL) was reacted with BA8OH (17 mg) in the presence of HATU (13 mg) with DIEA (9 μL) at 0 °C for 10 min and thereafter at 25 °C for 24 h. After removal of the solvent, the remaining solid was dissolved in chloroform and washed with 4 wt % $NaHCO_3$ aqueous solution and 4 wt % $NaHSO_4$ aqueous solution. The solvent was removed, and the remaining solid was purified by a Sephadex LH-20 column using methanol as eluant (17 mg, 65.1% yield). TLC: R_f(A) = 0.25, R_f(C) = 0.61. ^{1}H NMR (270 MHz, CDCl$_3$): δ (ppm) 1.11 (3H, t, COOCH$_2$CH_3), 1.38−1.55 (66H, brm, NHCH(CH_3)CONHC(CH_3)$_2$, NCH$_2$CH_3, (CH_3)$_3$C), 3.24 (2H, d, NHCHCH_2), 3.82, 3.95 (6H, m, NHCH(CH$_3$)CONHC(CH$_3$)$_2$), 4.06 (2H, q, COOCH_2CH$_3$), 4.32 (2H, q, NCH_2CH$_3$), 4.80 (1H, q, NHCHCH$_2$), 5.92 (1H, d, NHCHCH$_2$), 7.10−8.10 (19H, carbazolyl-*H*, NHCH(CH$_3$)CONHC(CH$_3$)$_2$). MS (FAB, matrix; nitrobezyl alcohol): *m*/*z* 1370 (calcd for $C_{66}H_{102}N_{14}O_{16}Na_1$ [(M + Na)$^+$] *m*/*z* 1369.76).

SS-A12-ECz. The Boc group of BA12-ECzAla-OEt (17 mg) was removed by treatment with 4 N HCl in dioxane, and the product dissolved in chloroform (1 mL) was reacted with DL-α-lipoic acid (5 mg) in the presence of HATU (14 mg) with DIEA (10 μL) at 0 °C for 10 min and thereafter at 25 °C for 24 h. After removal of the solvent, the remaining solid was dissolved in chloroform and washed with 4 wt % $NaHCO_3$ aqueous solution and 4 wt % $NaHSO_4$ aqueous solution. The solvent was removed and the remaining solid was purified by a Sephadex LH-20 column using methanol as eluant (6 mg, 33.3% yield). TLC: R_f(A) = 0.43, R_f(C) = 0.89. ^{1}H NMR (270 MHz, CDCl$_3$): δ (ppm) 1.10 (3H, t, COOCH$_2$CH_3), 1.35−1.62 (63H, brm, NHCH(CH_3)CONHC(CH_3)$_2$, NCH$_2$CH_3, CH$_2$(CH_2)$_3$CHCH$_2$CH$_2$SS), 1.80, 2.40 (2H, m, CH$_2$(CH$_2$)$_3$CHCH_2CH$_2$SS), 2.38 (2H, brs, CH_2(CH$_2$)$_3$CHCH$_2$CH$_2$SS), 3.12 (2H, m, CH$_2$(CH$_2$)$_3$CHCH$_2$CH_2SS), 3.32 (2H, d, NHCHCH_2), 3.48 (1H, m, CH$_2$(CH$_2$)$_3$CHCH$_2$CH$_2$SS), 3.94, 4.10 (6H, m, NHCH(CH$_3$)CONHC(CH$_3$)$_2$), 4.06 (2H, q, COOCH_2CH$_3$), 4.32 (2H, q, NCH_2CH$_3$), 4.70 (1H, q, NHCHCH$_2$), 7.12−8.15 (20H, carbazolyl-*H*, NHCH(CH$_3$)CONHC(CH$_3$)$_2$, NHCHCH$_2$). MS (FAB, matrix; nitrobezyl alcohol): *m*/*z* 1458 (calcd for $C_{69}H_{106}N_{14}O_{15}S_2Na_1$ [(M + Na)$^+$] *m*/*z* 1457.74).

BA20-SS. The Boc group of BA12-SS (67 mg) was removed by treatment with 4 N HCl in dioxane, and the product dissolved in chloroform (3 mL) was reacted with BA8OH (60 mg) in the presence of HATU (46 mg) with DIEA (32 μL) at 0 °C for 10 min and thereafter at 25 °C for 24 h. After removal of the solvent, the remaining solid was dissolved in chloroform and washed with 4 wt % $NaHCO_3$ aqueous solution and 4 wt % $NaHSO_4$ aqueous solution. The solvent was removed and the remaining solid was purified by a Sephadex LH-20 column using methanol as eluant (101 mg, 53.9% yield). TLC: R_f(A) = 0.43, R_f(C) = 0.85. ^{1}H NMR (270 MHz, CDCl$_3$): δ (ppm) 1.31−1.70 (107H, brm, NHCH(CH_3)CONHC(CH_3)$_2$, NHCH$_2$CH_2CH_2CH_2CH_2, (CH_3)$_3$C), 1.87, 2.41 (2H, m, CHCH_2CH$_2$SS), 3.07−3.14 (4H, brm, CHCH$_2$CH_2SS, NHCH_2CH$_2$CH$_2$CH$_2$CH$_2$), 3.52 (1H, m, CHCH$_2$CH$_2$SS), 3.93, 4.27 (10H, m, NHCH(CH$_3$)CONHC(CH$_3$)$_2$), 6.86 (1H, s, NHCH$_2$CH$_2$CH$_2$CH$_2$CH$_2$), 7.46−8.03 (20H, brm, NHCH(CH$_3$)CONHC(CH$_3$)$_2$).

ECz-A20-SS. The Boc group of BA20-SS (54 mg) was removed by treatment with 4 N HCl in dioxane, and the product dissolved in chloroform (4 mL) was reacted with Boc-ECzAla (17 mg) in the presence of HATU (25 mg) with DIEA (17 μL) at 0 °C for 10 min and thereafter at 25 °C for 24 h. After removal of the solvent, the remaining solid was dissolved in chloroform and washed with 4 wt % $NaHCO_3$ aqueous solution and 4 wt % $NaHSO_4$ aqueous solution. The solvent was removed and the remaining solid was purified by a Sephadex LH-20 column using methanol as eluant (45 mg, 72.6% yield). TLC: R_f(A) = 0.45, R_f(C) = 0.90. ^{1}H NMR (270 MHz, CDCl$_3$): δ (ppm) 1.35−1.58 (110H, brm, NHCH(CH_3)CONHC(CH_3)$_2$, NHCH$_2$CH_2CH_2CH_2CH_2, (CH_3)$_3$C, NCH$_2$CH_3,), 1.73, 2.35 (2H, m, CHCH_2CH$_2$SS), 2.97 (2H, m, CHCH$_2$CH_2SS), 3.15−3.30 (4H, brm, NHCH_2CH$_2$CH$_2$CH$_2$CH$_2$, NHCHCH_2), 3.52 (1H, m, CHCH$_2$CH$_2$SS), 3.93, 4.30 (10H, m, NHCH(CH$_3$)CONHC(CH$_3$)$_2$), 4.20 (2H, q, NCH_2CH$_3$), 4.28 (1H, q, NHCHCH$_2$), 5.92 (1H, s, NHCH$_2$CH$_2$CH$_2$CH$_2$CH$_2$), 7.30−8.12 (28H, brm, NHCH(CH$_3$)CONHC(CH$_3$)$_2$, NHCHCH$_2$, carbazolyl-*H*). MS (FAB, matrix; nitrobezyl alcohol): *m*/*z* 2139 (calcd for $C_{100}H_{161}N_{23}O_{23}S_2Na_1$ [(M + Na)$^+$] *m*/*z* 2139.16).

***N*,*N*-Bis(1-hydroxy-*n*-undecyl)amine.** 1-Amino-11-hydroxyundecane (480 mg) and 1-bromo-11-hydroxyundecane (643 mg) were dissolved in ethanol (20 mL), and the solution was refluxed at 80 °C for 24 h in the presence of K_2CO_3 (1060 mg). After removal of K_2CO_3 by filtration, the solvent was removed and the remaining solid was purified by a Sephadex LH-20 column using methanol as eluant (255 mg, 27.8% yield). TLC: R_f(B) = 0.29, R_f(D) = 0.48. ^{1}H NMR (270 MHz, CDCl$_3$): δ (ppm) 1.25 (28H, brs, NHCH$_2$CH$_2$(CH_2)$_7$CH$_2$CH$_2$OH), 1.53 (8H, m, NHCH$_2$CH_2(CH$_2$)$_7$CH$_2$CH_2OH), 2.53 (4H, t, NHCH_2CH$_2$(CH$_2$)$_7$CH$_2$CH$_2$OH), 3.60 (4H, t, NHCH$_2$CH$_2$(CH$_2$)$_7$CH$_2$CH_2OH).

***N*-(*tert*-Butyloxycarbonyl)-*N*,*N*-bis(1-hydroxy-*n*-undecyl)amine.** *N*,*N*-Bis(1-hydroxy-*n*-undecyl)amine (234 mg) and di-*tert*-butyl carbonate (171 mg) were dissolved in chloroform (10 mL), and the solution was stirred at room temperature for 4 h. The solvent was removed, and a crude product was obtained (317 mg, quantitative yield). TLC: R_f(B) = 0.54, R_f(D) = 0.79. ^{1}H NMR (270 MHz, CDCl$_3$): δ (ppm) 1.24 (28H, brs, NCH$_2$CH$_2$(CH_2)$_7$CH$_2$CH$_2$OH), 1.46 (9H, s, (CH$_3$)$_3$C), 1.53 (8H, m, NCH$_2$CH_2(CH$_2$)$_7$CH_2CH$_2$OH), 3.10 (4H, t, NCH_2CH$_2$(CH$_2$)$_7$CH$_2$CH$_2$OH), 3.61 (4H, t, NCH$_2$CH$_2$(CH$_2$)$_7$CH$_2$CH_2OH).

***N*-(*tert*-Butyloxycarbonyl)-*N*,*N*-bis(1-bromo-*n*-undecyl)amine.** *N*-(*tert*-Butyloxycarbonyl)-*N*,*N*-bis(1-hydroxy-*n*-undecyl)amine (200 mg) was reacted with 1,1′-carbonyl-bis-1*H*-imidazole (70 mg) in acetonitrile (10 mL) at room temperature for 30 min. Allyl bromide (7.6 mL) was added, and the solution was refluxed at 70 °C for 4 h. After removal of solvent, the reaction product was dissolved in chloroform and washed with 10 wt % aqueous citric acid solution and saturated aqueous NaCl solution. The solvent was evaporated, and the reaction product was obtained (154 mg, 60.4% yield). TLC: R_f(B) = 0.91, R_f(D) = 0.94. ^{1}H NMR (270 MHz, CDCl$_3$): δ (ppm) 1.24 (28H, brs, NCH$_2$CH$_2$(CH_2)$_7$CH$_2$CH$_2$Br), 1.46 (9H, s, (CH$_3$)$_3$C), 1.53 (8H, m, NCH$_2$CH_2(CH$_2$)$_7$CH_2CH$_2$Br), 3.11 (4H, t, NCH_2CH$_2$(CH$_2$)$_7$CH$_2$CH$_2$Br), 3.37 (4H, t, NCH$_2$CH$_2$(CH$_2$)$_7$CH$_2$CH_2Br).

1-(*tert*-Butyloxycarbonyl)-1-aza-13,14-dithiacyclopentacosane. *N*-(*tert*-Butyloxycarbonyl)-*N*,*N*-bis(1-bromo-*n*-undecyl)amine (40 mg) was reacted with sodium hydrosulfide (77 mg) in ethanol (10 mL) at room temperature for 24 h. The solution was neutralized with acetic acid/ethanol (1/10 v/v), iodide (22 mg) was added, and the solution was stirred at room temperature for 6 h. After evaporation of solvent, chloroform was added and the insoluble solid was removed. The solvent was removed, and the reaction product was obtained (27 mg, 80.9% yield). TLC: R_f(B) = 0.87, R_f(D) = 0.91. ^{1}H NMR (270 MHz, CDCl$_3$): δ (ppm) 1.24 (28H, brs, NCH$_2$CH$_2$(CH_2)$_7$CH$_2$CH$_2$SS), 1.46 (13H, brs, (CH_3)$_3$C, NCH$_2$CH_2(CH$_2$)$_7$CH$_2$CH$_2$SS), 1.53 (4H, m, NCH$_2$CH$_2$(CH$_2$)$_7$CH_2CH$_2$SS), 2.65 (4H, t, NCH$_2$CH$_2$(CH$_2$)$_7$CH$_2$CH_2SS), 3.10 (4H, t, NCH_2CH$_2$(CH$_2$)$_7$CH$_2$CH$_2$SS).

ECz-C11-SS. The Boc group of 1-(*tert*-butyloxycarbonyl)-1-aza-13,14-dithiacyclopentacosane (26 mg) was removed by treatment with 4 N HCl in dioxane, and the product dissolved in chloroform (1 mL) was reacted with Boc-ECzAla (24 mg) in the presence of HATU (36 mg) with DIEA (25 μL) at 0 °C for 10 min and thereafter at 25 °C for 12 h. After concentration of the solution, methanol was added to precipitate the reaction product and the product was purified by a Sephadex LH-20 column using tetrahydrofuran as eluant (19 mg, 47.8% yield). TLC: R_f(B) = 0.78, R_f(C) = 0.93. ^{1}H NMR (270 MHz, CDCl$_3$): δ (ppm) 1.25 (28H, brs, NCH$_2$CH$_2$(CH_2)$_7$CH$_2$CH$_2$SS), 1.40 (16H, brs, NCH$_2$CH_2(CH$_2$)$_7$CH$_2$CH$_2$SS, NCH$_2$CH_3, (CH_3)$_3$C), 1.57 (4H, m, NCH$_2$CH$_2$(CH$_2$)$_7$CH_2CH$_2$SS), 2.66 (4H, t, NCH$_2$CH$_2$(CH$_2$)$_7$CH$_2$CH_2SS), 2.83 (4H, brs, NCH_2CH$_2$(CH$_2$)$_7$CH$_2$CH$_2$SS), 3.13 (2H, d, NHCHCH_2), 4.30 (2H, q, NCH_2CH$_3$), 4.80 (1H, q, NHCHCH$_2$), 5.41 (1H, d, NHCHCH$_2$), 7.20−8.14 (7H, carbazolyl-*H*). MS (FAB, matrix; nitrobezyl alcohol + thioglycerol): *m*/*z* 753 (calcd for $C_{44}H_{70}N_3O_3S_2$ [(M + H)$^+$] *m*/*z* 752.48), *m*/*z* 860 (calcd for $C_{47}H_{78}N_3O_5S_3$ [(M + thioglycerol + H)$^+$] *m*/*z* 860.50), *m*/*z* 966 (calcd for $C_{50}H_{86}N_3O_7S_4$ [(M + two × thioglycerol + H)$^+$] *m*/*z* 968.53).

Circular Dichroism (CD) Measurements. CD spectra of the peptides were measured in a methanol solution at 20 °C on a CD spectrometer (J-600, JASCO Co., Ltd., Japan) using an optical cell of 1 cm path length.

Preparation of Self-Assembled Monolayers. A substrate coated

with gold was prepared by vapor deposition of chrominium and then gold (99.99%) onto a clean slide glass. The thickness of the chrominium and gold layers, monitored by a quartz oscillator, were approximately 100 and 1000 Å, respectively. In advance of the vapor deposition, the slide glass was treated with methanol, distilled water, and H_2SO_4 (97%): H_2O_2 (30%) = 7:3 (a piranha solution) for 3 h. The plate was washed thoroughly with distilled water and methanol. The gold substrate was used for a self-assembling experiment within a few days of preparation. The gold substrate was incubated in an ethanol solution of a disulfide compound (0.1 mM) for 24 h. After the incubation, the substrate was rinsed rigorously with ethanol and dried in stream of dry nitrogen gas.

Quartz Crystal Microbalance (QCM) Measurements. QCM is known to be very sensitive mass measuring device.[24,25] The QCM employed is a commercially available 9 MHz, AT-cut quartz (diameter 9 mm), purchased from USI Co., Ltd. (Japan). The quartz-crystal plates with Au deposited on both sides were used. The 9 MHz QCM was connected to a oscillator (Q-200S, USI Co., Ltd., Japan). The frequency changes were followed by a universal counter (model 53131A, Hewlett-Packard Co., Ltd., CA). The following equation (eq 1) has been established for an AT-cut shear mode QCM.[26]

$$\Delta F = \frac{-2F_0^{\,2}}{A\sqrt{\rho_q \mu_q}}\Delta m \qquad (1)$$

ΔF, F_0, Δm, A, ρ_q, and μ_q represent the measured frequency shift (Hz), the fundamental frequency of the QCM (9×10^6 Hz), the mass change (g), the electrode area (0.16 cm^2), the density of the quartz (2.65 g cm^{-3}), and the shear modulus of the quartz (2.95×10^{11} dyn cm^{-2}), respectively. The both sides of the Au electrode of the QCM were washed with a piranha solution in order to remove organic adsorbate impurities from the gold surfaces. The QCM was rinsed with Milli-Q water and methanol, and dried in a vacuum. The QCM was immersed into an ethanol solution of a disulfide compound (0.1 mM) for 3−5 h. After washing with ethanol, the QCM was dried in the air, and the mass change was calculated from the frequency shift using eq 1.

Cyclic Voltammetry. Cyclic voltammograms were obtained using a voltammetric analyzer (model 604, BAS Co., Ltd., Japan) at room temperature. A standard three-electrode configuration was used with a gold-coated substrate as the working electrode, Ag/AgCl as the reference electrode, and a platinum wire as the auxiliary electrode in a glass vessel. All of the electric potentials reported in this paper were measured with respect to the reference electrode. The area of the working electrode exposed to the electrolyte solution was 0.90 cm^2. The redox reagent used for blocking experiments was 1 mM $K_3[Fe(CN)_6]$ in 1 M KCl analyte solution. The sweep rate was set at 50 mV s^{-1} for all measurements.

Impedance Spectroscopy. Impedance measurements were carried out in the frequency range of 100 kHz to 0.01 Hz with an amplitude of 50 mV and fixed static potential of −0.5 V with the three-electrode setup described above under nitrogen atmosphere at room temperature. The supporting electrolyte used was Na_2SO_4 (0.01 M). The results were presented as Bode plots and Nyquist plots and analyzed by comparing the experimental data with a model equivalent circuit consisting of a resistor in series with a parallel capacitor/resistor combination that generally corresponds to the monolayer.

Fourier Transform Infrared Reflection−Absorption Spectroscopy (FTIR-RAS). The FTIR spectra were recorded on a Fourier transform infrared spectrometer (Magna 850, Nicolet Japan Co., Ltd., Japan) at room temperature. For RAS measurements, a reflection attachment (model RMA-1DG/VRA, Harrick Co., Ltd., NY) was used, and a *p*-polarized beam was obtained through an Au/AuBr wire-grid polarizer (Hitachi Co., Ltd., Japan). The incident angle was set at 85° from the surface normal. The number of interferogram accumulations was 500. Molecular orientation of the peptide monolayer on a gold surface was determined on the basis of the amide I/amide II absorbance ratio in the FTIR−RAS spectrum according to eq 2 under the assumption of a uniform crystal of the peptide-thin layer.[19,27−31]

$$\frac{I_1}{I_2} = 1.5 \times \frac{(3\cos^2\gamma - 1)(3\cos^2\theta_1 - 1) + 2}{(3\cos^2\gamma - 1)(3\cos^2\theta_2 - 1) + 2} \qquad (2)$$

I_i, γ, and θ_i ($i = 1$ or 2 corresponding to amide I or amide II) represent the observed absorbance, the tilt angle of the helix axis from the surface normal, and the angle between the transition moment and the helix axis, respectively. The values of the θ_1 and θ_2 are taken to be 39° and 75°, respectively.[32]

Photocurrent Generation Experiments. Photocurrent measurements were carried out using the three-electrode setup described above at room temperature. The supporting electrolyte used was Na_2SO_4 (0.1 M). The SAM-modified electrodes were photoirradiated with a Xe lamp (500 W, JASCO Co., Ltd., Japan) equipped with a monochromator. The photocurrents generated from the SAM electrodes were detected by the voltammetric analyzer described above. The concentrations of an electron acceptor (MV^{2+}) and electron donors (TEOA, EDTA) were set at 50 mM. The intensity of the incident light was evaluated by a potassium ferrioxalate actinometry.[33,34] The quantum efficiency of the photocurrent generation (the number of electron flowed upon photoirradiation/the number of photon absorbed by ECz groups) was determined at light intensity of 4.73×10^{-11} einstein s^{-1} for 299 nm excitation and 1.25×10^{-10} einstein s^{-1} for 351 nm excitation, respectively. The number of photons absorbed by ECz groups was calculated from the absorbance of the SAMs, which were derived from the surface coverage assuming that the molar absorptivities of the SAMs are the same as those of the disulfide compounds in a chloroform solution.

Results and Discussion

Conformation of Peptides in Solution. The CD spectra of the peptides carrying an ECz group and a disulfide group in a methanol solution are shown in Figure 2. These tridecapeptides and heneicosapeptide are designed to adopt α-helical conformation on the basis of the investigation of a series of $(Ala\text{-}Aib)_n$ peptides on the conformation.[17] All peptides show a double-minimum profile, which is characteristic of an α-helical structure.[35,36] The helix contents of ECz-A12-SS, SS-A12-ECz, and ECz-A20-SS were determined to be 45.4%, 49.2%, and 81.8%,[37] respectively, showing that the longer peptide chain stabilizes an α-helical conformation.

Surface Coverage of Self-Assembled Monolayers. The surface coverage of the SAMs prepared from the disulfide compounds was investigated by QCM measurements. Surface coverage of ECz-A12-SS, SS-A12-ECz, ECz-A20-SS, and ECz-C11-SS on a gold surface were 0.114, 0.145, 0.176, and 0.345 nmol cm^{-2}, respectively. The corresponding molecular areas are 146, 115, 94.4, and 48.1 $Å^2$/molecule, respectively, indicating that the SAM of a tridecapeptide connected to a gold surface at the C-terminal of the peptide covered a gold surface to a lesser extent than that of a tridecapeptide connected at the

(24) Muramatsu, H.; Dicks, J. M.; Tamiya, E.; Karube, I. *Anal. Chem.* **1987**, *59*, 2760.
(25) Okahata, Y.; Matsunobu, Y.; Ijiro, K.; Mukae, M.; Murakami, A.; Makino, K. *J. Am. Chem. Soc.* **1992**, *114*, 8299.
(26) Sauerbrey, G. *Z. Phys.* **1959**, *155*, 206.
(27) Greenler, R. G. *J. Chem. Phys.* **1966**, *44*, 310.
(28) Gremlich, H. U.; Fringeli, U. P.; Schwyzer, R. *Biochemistry* **1983**, *22*, 4257.
(29) Debe, M. K. *J. Appl. Phys.* **1984**, *55*, 3354.
(30) Okamura, E.; Umemura, J.; Takenaka, T. *Can. J. Chem.* **1991**, *69*, 1691.
(31) Worley, C. G.; Linton, R. W.; Samulski, E. T. *Langmuir* **1995**, *11*, 3805.
(32) Tsuboi, M. *J. Polym. Sci.* **1965**, *59*, 139.
(33) Parker, C. A. *Proc. R. Soc., Ser. A* **1956**, *235*, 518.
(34) Hatchard, C. G.; Parker, C. A. *Proc. R. Soc., Ser. A* **1956**, *235*, 518.
(35) Holzwarth, G.; Doty, P. *J. Am. Chem. Soc.* **1965**, *87*, 218.
(36) Greenfield, N.; Fasman, G. D. *Biochemistry* **1969**, *8*, 4108.
(37) Chen, Y. H.; Yang, J. T.; Martinez, H. M. *Biochemistry* **1972**, *11*, 4120.

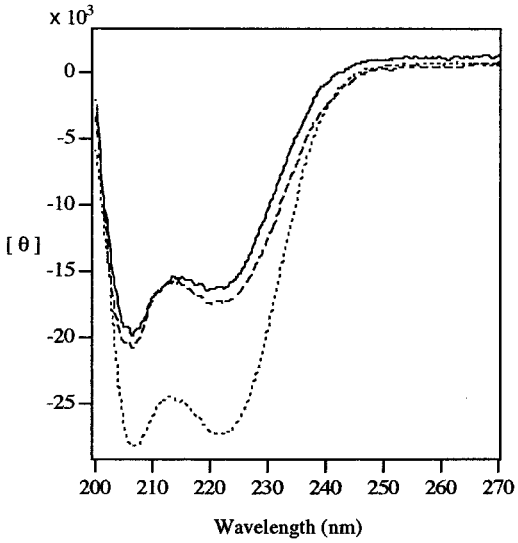

Figure 2. CD spectra of ECz-A12-SS (solid line), SS-A12-ECz (dashed line), and ECz-A20-SS (dotted line) in methanol at a concentration of 6.4×10^{-6} M at 20 °C.

N-terminal. A similar result was reported with the other peptide SAMs, where the peptide SAM connected to a gold surface via the N-terminal was more dense than the peptide SAM connected via the C-terminal.[38] This result is possibly due to unfavorable electrostatic repulsion between the dipoles of the helical peptide directing toward an aqueous phase and the dipoles of an S−Au linkage (S^--Au^+) opposing the helix dipoles.[39,40] However, we cannot exclude the other factors such as the chain-length difference at the anchor part of the molecules and the different size and polarity of the protecting terminal groups.

The SAM composed of a longer peptide, ECz-A20-SS, covered a gold surface more densely than the SAMs of the tridecapeptides, and the area per a unit molecule approached to the cross-section area of Boc-(Ala-Aib)$_4$-OMe, which is determined on the basis of X-ray crystal analysis.[17] A longer helix peptide seems to strengthen the aggregation of peptide molecules by van der Waals force in the SAM, resulting in the formation of a highly ordered monolayer.[19] The area per a unit molecule of ECz-C11-SS on a gold surface is much smaller than those of the helical peptides because of the smaller cross section of the dialkyl group and is nearly twice as large as that of a single-chain *n*-alkanethiol (22 Å^2/molecule).[41]

The prepared SAMs were studied by cyclic voltammetry. The cyclic voltammograms of a bare surface and the SAMs were measured in an aqueous $K_3[Fe(CN)_6]$ solution and are shown in Figure 3. With the exception of the ECz-A12-SS SAM, other SAMs did not show redox activity, indicating that these SAMs possess a well-packed monolayer structure and an insulating property. The redox peaks of ferricyanide observed in the case of the ECz-A12-SS SAM are smaller than those of a bare gold, showing that this monolayer possesses some defects or incompletely packed regions where the electrolyte can diffuse in. This result agrees well with the QCM observation.

The relative dielectric constants of the SAMs were determined by the impedance spectroscopy in an Na_2SO_4 solution.[42−45] The measurements were carried out at a potential of −0.5 V, where no redox reaction occurs. The capacitance values for the ECz-A12-SS, SS-A12-ECz, and ECz-C11-SS SAMs were calculated to be 5.01, 2.98, and 2.24 μF/cm^{-2}, respectively. Considering the monolayer as a plate condenser, the capacitance is defined by eq 3

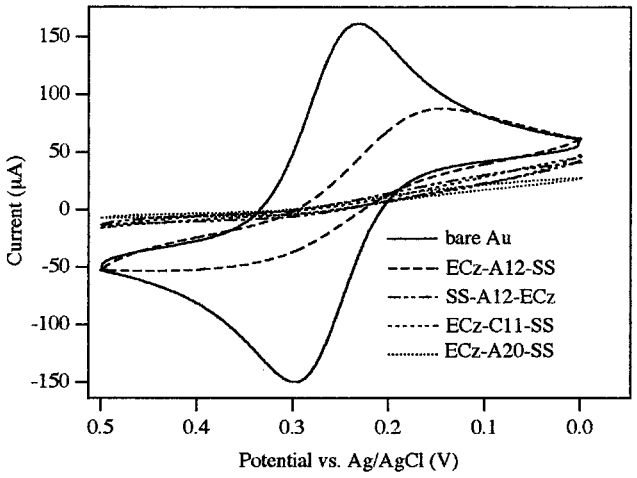

Figure 3. Cyclic voltammograms of a bare surface and the SAM-covered surfaces in a 1 mM aqueous $K_3[Fe(CN)_6]$ solution at room temperature. The sweep rate was set at 50 mV s^{-1}.

$$C_m = \frac{\epsilon_0 \epsilon_m}{d} \tag{3}$$

where C_m, ϵ_0, ϵ_m, and d represent the capacitance of the monolayer, the dielectric permittivity of free space, the relative dielectric constant of the monolayer, and the thickness of the monolayer, respectively. The thickness of the SAMs was calculated to be about 21 Å for the tridecapeptide SAMs and 17 Å for the ECz-C11-SS SAM on the basis of the molecular orientation on the gold surface (described in the following section). The ϵ_m values were calculated by eq 3 to be 12, 7.4, 4.3 for the ECz-A12-SS, SS-A12-ECz, and ECz-C11-SS SAMs, respectively. The dielectric constant of the ECz-A12-SS SAM is considerably high, indicating penetration of electrolytes or water molecules into the SAM through the defects.

Orientation of Helical Peptides on Gold Surface. The FTIR-RAS spectrum of the ECz-A12-SS SAM is shown in Figure 4. The absorptions observed at 1675 and 1538 cm^{-1} were assigned to amide I and amide II bands of an α-helical conformation,[46] respectively, indicating an α-helical structure for the peptide SAM. The amide I/amide II absorbance ratios of the ECz-A12-SS, SS-A12-ECz, and ECz-A20-SS SAMs were 2.34, 2.71, and 3.34, respectively. The corresponding tilt angles of the helices from the surface normal were calculated using eq 2 to be 44°, 41°, and 36°, respectively. The surface areas occupied by a molecule were calculated using these tilt angles to be 121, 114, and 105 Å^2/molecule for ECz-A12-SS, SS-A12-ECz, and ECz-A20-SS, respectively, assuming hexagonal packing of the helices and uniform orientation in the SAMs. The surface areas of the SS-A12-ECz and ECz-A20-SS SAMs determined by FTIR-RAS coincide with those obtained by the QCM measurements. On the other hand, the surface area of the

(38) Fujita, K.; Bunjes, N.; Nakajima, K.; Hara, M.; Sasabe, H.; Knoll, W. *Langmuir* **1998**, *14*, 6167.
(39) Nuzzo, R. G.; Fusco, F. A.; Allara, D. L. *J. Am. Chem. Soc.* **1987**, *109*, 2358.
(40) Biebuyck, H. A.; Whitesides, G. M. *Langmuir* **1993**, *9*, 1766.
(41) Strong, L.; Whitesides, G. M. *Langmuir* **1988**, *4*, 546.
(42) Plant, A. L.; Gueguetchkeri, M.; Yap, W. *Biophys. J.* **1994**, *67*, 1126.
(43) Gafni, Y.; Weizman, H.; Libman, J.; Shanzer, A.; Rubinstein, I. *Chem. Eur. J.* **1996**, *2*, 759.
(44) Steinem, C.; Janshoff, A.; Ulrich, W.-P.; Sieber, M.; Galla, H.-J. *Biochim. Biophys. Acta* **1996**, *1279*, 169.
(45) Motesharei, K.; Ghadiri, M. R. *J. Am. Chem. Soc.* **1997**, *119*, 11306.
(46) Kennedy, D. F.; Chrisma, M.; Chapman, T. D. *Biochemistry* **1991**, *30*, 6541.

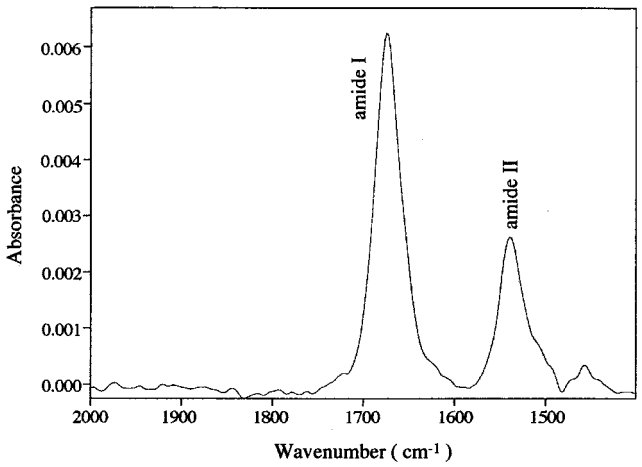

Figure 4. FTIR-RAS spectrum of the ECz-A12-SS SAM.

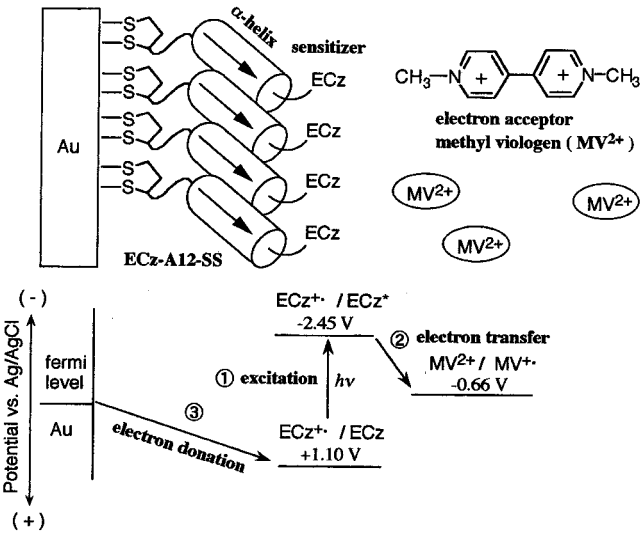

Figure 5. Schematic illustration of cathodic photocurrent generation by the α-helical peptide SAM in the presence of MV^{2+}.

ECz-A12-SS SAM from FTIR-RAS was slightly smaller than that from the QCM measurement (146 $Å^2$/molecule). The ECz-A12-SS SAM should contain some defects or incompletely packed regions, which is agreeable with the results from the cyclic voltammetry and impedance spectroscopy.

Cathodic Photocurrent Generation by Self-Assembled Monolayers. Photocurrent generation by the SAMs was investigated in an aqueous MV^{2+} solution. The mechanism of the cathodic photocurrent generation by the SAMs is presented schematically in Figure 5. Upon photoexcitaion of an ECz group, electron transfer occurs from the excited ECz group to an electron acceptor MV^{2+}, followed by electron donation from a gold surface to the oxidized ECz group (the radical cation of the ECz group). The reduced viologen diffuses to the auxiliary electrode and transfers an electron, resulting in the generation of a photocurrent. The measured photocurrents generated by photoirradiation of the SAMs with a monochromic light of 351 nm (10 nm bandwidth) are shown in Figure 6 with repeating on−off switchings of the photoirradiation (irradiation duration was 30 s).

The largest photocurrent was observed in the ECz-C11-SS SAM. The photocurrent of the ECz-A12-SS SAM was nearly equal to that of the SS-A12-ECz SAM. However, since the density of the ECz group is not the same in these SAMs, the quantum efficiencies of the cathodic photocurrent generation were calculated and summarized in Table 1. The tridecapeptide

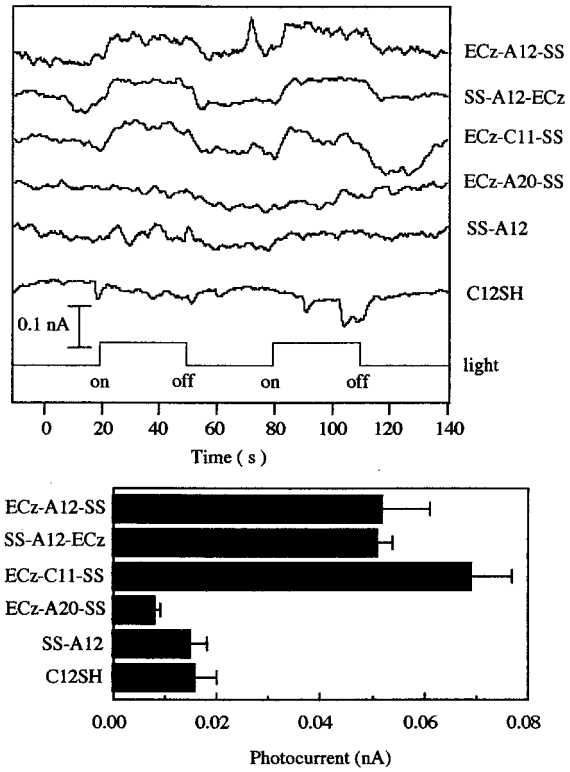

Figure 6. Time course of the photocurrents of the SAMs in an aqueous MV^{2+} solution at 0 V upon photoirradiation at 351 nm (1.25×10^{-10} einstein s^{-1}) at room temperature (top). Photocurrents of the SAMs (bottom).

Table 1. Quantum Efficiency of the Cathodic Photocurrent Generation in an Aqueous MV^{2+} Solution and the Anodic Photocurrent Generation in an Aqueous TEOA or EDTA Solution

	MV^{2+} (%)	TEOA (%)	EDTA (%)
ECz-A12-SS	0.43	0.19	0.17
SS-A12-ECz	0.33	0.45	0.42
ECz-C11-SS	0.19	0.10	0.04
ECz-A20-SS	0.04	0.07	0.03

SAMs show higher quantum efficiencies than the ECz-C11-SS SAM. In addition, the efficiency of the ECz-A12-SS SAM where the dipole of α-helix directs toward an aqueous phase so as to accelerate the electron donation from a gold surface to an ECz group was higher than that of the SS-A12-ECz SAM having the dipole moment reverse-directed to that in the ECz-A12-SS SAM. The difference in the efficiencies is, however, too small to be explained by the dipole effect of the peptide. The ECz-A12-SS SAM contains structural defects to allow the electrolytes and water to penetrate in, which may weaken the dipole effect in the monolayer.

A photocurrent was slightly observed in the ECz-A20-SS SAM (Figure 6). The distance between a gold surface and an ECz group in the SAM is calculated to be about 41 Å, which is the sum of the lipoic part (9.6 Å, upon all-trans configuration) and the helical peptide part (31.5 Å). The molecular length of the ECz-A20-SS chain is too long for efficient electron transfer by the through bond mechanism to occur. The SS-A12 and C12SH SAMs which lack ECz group did not generate a significant photocurrent, showing that the photoexcitation of an ECz group initiates the photocurrent generation. In addition, the action spectrum of the photocurrent of the ECz-C11-SS SAM agrees well with the absorption spectrum of ECz-C11-SS in a chloroform solution, indicating that ECz group is the photosensitizing species (Figure 7).

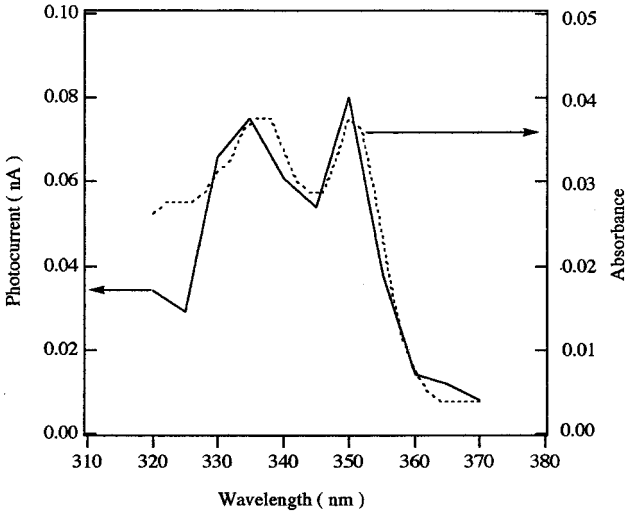

Figure 7. Photocurrent action spectrum of the ECz-C11-SS SAM (solid line) and the absorption spectrum of ECz-C11-SS in chloroform (dotted line).

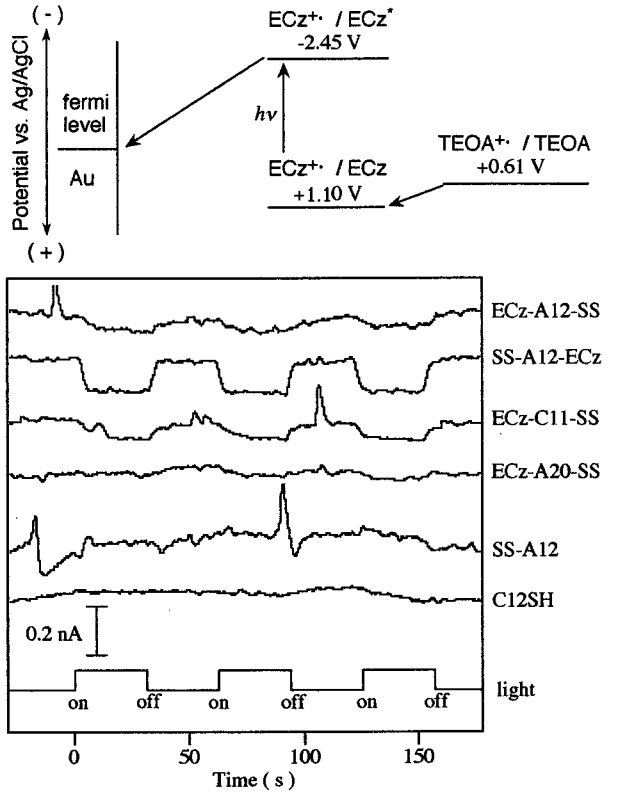

Figure 8. Energy diagram for anodic photocurrent generation in the presence of TEOA (top). Time course of the photocurrent of the SAMs in an aqueous TEOA solution at 0 V upon photoirradiation at 299 nm (4.73×10^{-11} einstein s^{-1}) at room temperature (bottom).

Anodic Photocurrent Generation by Self-Assembled Monolayers. Anodic photocurrent generation by the SAMs was investigated in the presence of an electron donor, TEOA or EDTA. The photocurrents generated upon photoirradiation with a monochromic light of 299 nm (10 nm bandwidth) in the presence of TEOA are shown in Figure 8. The observed photocurrents are summarized in Figure 9. The largest photocurrent was obtained in the SS-A12-ECz SAM, and the small currents were obtained in the ECz-A12-SS and ECz-C11-SS SAMs. The quantum efficiencies of the anodic photocurrents are also summarized in Table 1. The large quantum efficiency of the SS-A12-ECz SAM is possibly due to the helix dipole

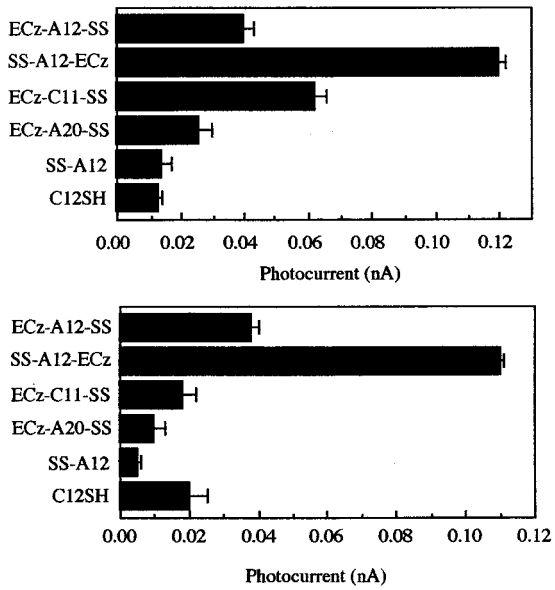

Figure 9. Anodic photocurrent of the SAMs in an aqueous TEOA (top) or EDTA solution (bottom) at 0 V upon photoirradiation at 299 nm at room temperature.

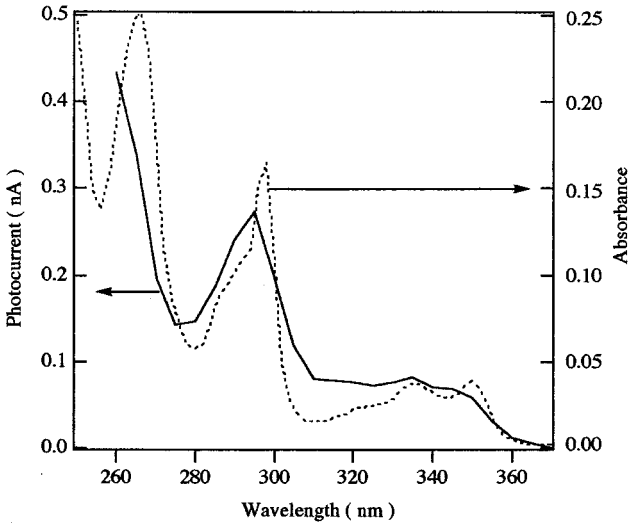

Figure 10. Photocurrent action spectrum of the SS-A12-ECz SAM (solid line) and the absorption spectrum of SS-A12-ECz in methanol (dotted line).

directing toward a gold surface, significantly accelerating electron transfer from an ECz group to a gold surface (This point is discussed in the last section). The action spectrum of the SS-A12-ECz SAM was also measured and is shown to agree with the absorption spectrum of SS-A12-ECz in a methanol solution (Figure 10).

Electronic Coupling through Helical Peptides. To investigate the mediation of electron transfer by peptide molecules, the dependence of the quantum efficiency for the anodic photocurrent generation on the electric potential was investigated using EDTA as an electron donor (Figure 11). In all the SAMs, a decrease in the anodic photocurrent was observed with an increase of the negative bias to the working electrode, and the photocurrent disappeared at a certain potential (zero-current potential). The negative bias reduces the energy gap between the oxidation potential of an excited ECz group and the Fermi level of gold, resulting in the decrease of anodic photocurrent. The anodic photocurrent was changed to a cathodic photocurrent by applying the negative bias larger than the zero-current

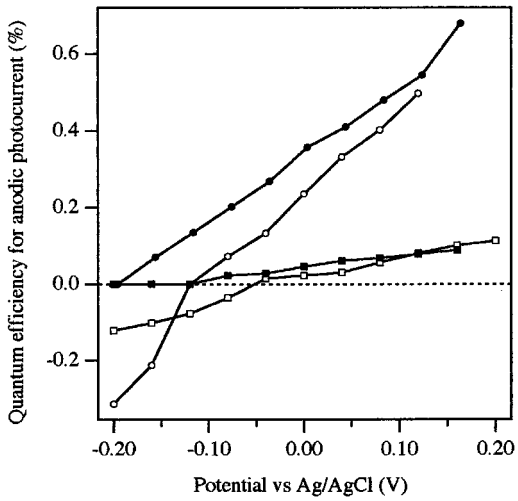

Figure 11. Effect of electric potential on the anodic photocurrent generation using EDTA in the ECz-A12-SS (○), SS-A12-ECz (●), ECz-A20-SS (■), and ECz-C11-SS (□) SAMs.

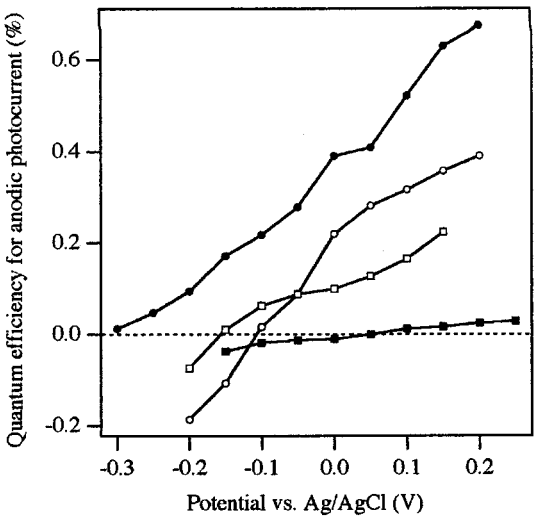

Figure 12. Effect of electric potential on the anodic photocurrent generation using TEOA in the ECz-A12-SS (○), SS-A12-ECz (●), ECz-A20-SS (■), and ECz-C11-SS (□) SAMs.

potential. A specific electron acceptor, such as H^+ in an aqueous solution, may accept an electron from a photoexcited ECz group to generate the cathodic photocurrent. Therefore, the observed photocurrent should be the sum of anodic and cathodic photocurrents. At the zero-current potential, the opposing photocurrents cancel each other, leading apparently to a no-current state.

An anodic photocurrent generation, using EDTA as an electron donor, is composed of two electron-transfer steps: from EDTA to a photoexcited ECz group and from a radical anion of the ECz group to a gold surface. The latter should be the rate-limiting step because of the long distance between the donor and acceptor. Thus the quantum efficiency of the photocurrent generation should be influenced directly by the rate constant for the latter electron transfer. The rate constant of electron transfer (k_{ET}) from a donor to an acceptor at a fixed distance is described by eq 4 on the basis of the semiclassical theory.[47] The present data are discussed in terms of eq 4, because it is essentially the same as the equation for the electron transfer on a metal surface.[48−50]

$$k_{ET} = \sqrt{\frac{4\pi^3}{h^2 \lambda k_B T}} H_{DA}{}^2 \exp\left[-\frac{(\Delta G_0 + \lambda)^2}{4\lambda k_B T}\right] \qquad (4)$$

$$H_{DA}{}^2 = (H_{DA}{}^0)^2 \exp(-\beta r)$$

h, λ, k_B, T, $H_{DA}{}^2$, $(H_{DA}{}^0)^2$, ΔG_0, β, and r represent Planck's constant, the reorganization energy, the Boltzmann's constant, the absolute temperature, the electronic coupling strength between donor and acceptor, the coupling strength at the closest contact, the driving force for the reaction, the tunneling parameter for the medium, and the edge-to-edge distance between donor and acceptor groups, respectively. On the basis of the simple model where the peptide dipole influences only the electric potential around an ECz groups, the driving force in the electron transfer in each SAM is the same at the relative potential to the zero-current potential. According to eq 4, k_{ET} is proportional to $H_{DA}{}^2$ under the same driving force (ΔG_0). Therefore, the difference in the quantum efficiencies of the photocurrent generation can be explained in terms of $H_{DA}{}^2$. The relationship between the quantum efficiency of the photocurrent generation and the electric potential appears to be linear (Figure 11). The slope for the tridecapeptide SAM was larger than that for the ECz-C11-SS SAM, indicating that the electronic coupling strength in the peptide SAM should be larger than that in the ECz-C11-SS SAM. This difference can be understood in terms of different tunneling parameters for electron-transfer medium (β). The donor (ECz group)−acceptor (gold surface) distance along the molecular axis is calculated to be 29 Å (ECz-A12-SS), 28 Å (SS-A12-ECz), and 41 Å (ECz-A20-SS) for a fully helical conformation of peptides, and 20 Å for all trans forms of ECz-C11-SS. When the β value for ECz-C11-SS is taken to be 0.9 $Å^{-1}$ according to the reported value for alkanes,[51] the β values are calculated to be 0.58 $Å^{-1}$ (ECz-A12-SS), 0.60 $Å^{-1}$ (SS-A12-ECz), and 0.46 $Å^{-1}$ (ECz-A20-SS). Therefore, the peptide molecule is a better medium for electron transfer than a saturated hydrocarbon by about 40% reduction of the β value. However, the ECz-A12-SS SAM contains electrolytes and water molecules in the monolayer as shown by the cyclic voltammetry and impedance spectroscopy. Therefore, the β value for the ECz-A12-SS remains uncertain, although the value is in accordance with that in the SS-A12-ECz SAM.

The Effect of Dipole Moment on Photocurrent Generation. To clarify whether the peptide dipole accelerates electron transfer in the SAMs, the dependence on the electric potential of the quantum efficiency for the anodic photocurrent generation using TEOA as an electron donor was investigated (Figure 12). In the case of all the SAMs, a decrease in the anodic photocurrent was observed with an increase of the negative bias to the working electrode as observed in the case of using EDTA as an electron donor. The zero-current potentials for the ECz-A12-SS, SS-A12-ECz, ECz-A20-SS, and ECz-C11-SS SAMs are −0.11 V, −0.30 V, +0.05 V, and −0.16 V, respectively. The SS-A12-ECz SAM shows a negative potential shift from that for the ECz-C11-SS SAM (−0.14 V). On the other hand, a positive potential shift from that for the ECz-C11-SS SAM was observed for the ECz-A12-SS SAM (+0.05 V) or for the ECz-A20-SS SAM (+0.21). These shifts are therefore explain-

(47) Marcus, R. A.; Sutin, N. *Biochim. Biophys. Acta* **1985**, *811*, 265.
(48) Weber, K.; Hockett, L.; Creager, S. E. *J. Phys. Chem. B* **1997**, *101*, 8286.
(49) Chidsey, C. E. D. *Science* **1991**, *251*, 919.
(50) Zusman, L. D. *Chem. Phys.* **1987**, *112*, 53.
(51) Creager, S.; Yu, C. J.; Bamdad, C.; O'Connor, S.; Maclean, T.; Lam, E.; Chong, Y.; Olsen, G. T.; Luo, J.; Gozin, M.; Kayyem, J. F. *J. Am. Chem. Soc.* **1999**, *121*, 1059.

able by the negative potential or the positive potential around the ECz group induced by the neighboring negative terminals or the positive terminals of the corresponding helical dipoles. The negative shift of the zero-current potential results in a large driving force for the photocurrent generation to accelerate the electron transfer from an ECz group to a gold surface. The expected potential shift induced by the dipole moment of the helical peptide (ϕ) can be calculated by eq 5,[52,53]

$$\phi = \frac{mn_a \cos \gamma}{\epsilon_0 \epsilon_m (1 + 9\alpha n_a^{3/2})} \quad (5)$$

where m, n_a, γ, ϵ_0, ϵ_m, and α represent the helix dipole moment, the number of peptide molecules per unit area, the tilt angle of helix axis from the surface normal, the dielectric permittivity of free space, the relative dielectric constant of the monolayer, and the polarizability of the peptide molecule, respectively. The dipole moment along the helix axis and the polarizability were calculated to be 42.0 D and 65.7 Å^3 for the tridecapeptide, and 71.6 D and 105.3 Å^3 for the heneicosapeptide by using MOPAC calculation. On the basis of eq 5, the ϕ values were calculated to be 0.49, −0.95, and 1.5 V for the ECz-A12-SS, SS-A12-ECz, and ECz-A20-SS SAMs, respectively. However, these potentials induced by the dipole moment are reduced by the ionic property of the Au^+-S^- linkage[54] and/or the charge transfer from gold to the peptide layer.[53] Indeed, the surface potentials for the SAMs of Lipo-(Ala-Aib)$_8$-OBzl (Lipo and OBzl represent lipoic acid and benzyl ester, respectively) and Boc-(Ala-Aib)$_8$-LipoA (Boc and LipoA represent the *tert*-butyloxycarbonyl group and a lipoic acid derivative containing an amino group, respectively) were −0.12 and 0.40 V, respectively. The former value was explainable by calculation taking the ionic charge on the Au^+-S^- linkage into consideration. It is therefore predicted that the electric potential generated by the dipole moment of SS-A12-ECz and ECz-A20-SS will be slightly smaller magnitudes than these values. The differences of the zero-current potentials of the SS-A12-ECz SAM and the ECz-A20-SS SAM from the control SAM of ECz-C11-SS were, respectively, −0.14 and 0.21 V, which are thus agreeable semiquantitatively with the predicted values. In addition, the magnitude of the shift is proportional to the peptide chain length (13:21), indicating that the potential shift should arise from the dipole moment of the helical peptide. The β values were also calculated on the basis of the slope in Figure 12 to be 0.60, 0.62, and 0.48 Å^{-1} for the ECz-A12-SS, SS-A12-ECz, and ECz-A20-SS SAMs, respectively. These values are in good agreement with the results obtained in the EDTA system described above.

Conclusion

Self-assembled monolayers (SAMs) composed of helical peptides carrying an *N*-ethylcarbazolyl (ECz) group were prepared, and the quantum efficiencies of the photocurrent generation were investigated. The cathodic photocurrent generation experiments did not provide compelling evidence of the dipole effect. This is because the ECz-A12-SS SAM contains structural defects to allow the electrolyte, the cationic MV^{2+}, to diffuse in the monolayer, resulting in the cancelation of the dipole effect. To evaluate the dipole effect, the photocurrent generation of the SS-A12-ECz, ECz-A20-SS, and ECz-C11-SS SAMs, which formed tightly packed monolayers, were investigated using TEOA as an electron donor because of its electrically neutral property. The anodic photocurrent using TEOA was accelerated by the use of the helix peptide SAM with the helix dipole directing toward a gold surface. The difference in the zero-current potentials of the SAMs is explainable semiquantitatively by the electric potential produced by the dipole moment. The helix dipole therefore affects the electric potential around an ECz group, leading to the increase of the driving force for the electron transfer. Furthermore, the peptide molecules are shown to be better medium for electron transfer in the SAMs than saturated hydrocarbon as evidenced by the smaller β value.

Acknowledgment. This study is partly supported by Iketani Science and Technology Foundation.

JA992769L

(52) Knapp, A. G. *Surf. Sci*. **1973**, *34*, 289.
(53) Ito, E.; Iwamoto, M. *J. Appl. Phys.* **1997**, *81*, 1790.
(54) Miura, Y.; Kimura, S.; Kobayashi, S.; Iwamoto, M.; Imanishi, Y.; Umemura, J., *Chem. Phys. Lett.*, in press.